Optimal packing in 2D and 3D granular systems: Density, connectivity, and force distributions

William-Fernando Oquendo[1,2,*] and *Nicolas* Estrada[3,**]

[1]Universidad Nacional de Colombia, Sede Bogotá, Facultad de Ciencias, Departamento de Física, 111321 - Colombia
[2]Universidad de la Sabana, Facultad de Ingeniería, 140013 - Colombia
[3]Universidad de los Andes, Departamento de Ingeniería Civil y Ambiental, 111711 - Colombia

Abstract. In this work, we explore the influence of the grain size distribution (GSD) on density, connectivity and internal forces distributions, for both 2D and 3D granular packings built mechanically. For power law GSDs, we show that there is an exponent for which density and connectivity are optimized, and this exponent is close to those that characterize other well known GSDs such as the Fuller and Thompson distribution and the Appollonian packing. In addition, we studied the distributions of normal forces, finding that these can be well described by a power-law tail, specially for the GSDs with large size span. These results highlight the role of the GSD on internal structure and suggest important consequences on macroscopic properties.

1 Introduction

Packing materials optimally is an ancient problem with roots on the simple storage of agricultural and manufacturing products, and still has implications even on seemingly unrelated topics such as secure coding through the Kepler problem [1]. The meaning of the word "optimal" actually depends on the context. In our case we focus on the packing density, which constitutes a simple descriptor, with multiple applications in civil engineering such as concrete and pavements design.

In fact, packing granular materials is a relevant problem in various fields, and it has been approached in different types of research studies, for both frictionless [2–6] and frictional [3, 7–11] systems. For example, since more than a century civil engineers have studied grain size distributions (GSDs) in order to obtain the densest materials. Fuller and Thomson [12–16] found that a GSD of the form

$$\rho(d) = \left(\frac{d}{d_{\max}}\right)^{\eta}, \tag{1}$$

produces the densest material when the exponent $\eta \simeq 0.5$. Here ρ is the cumulative volume fraction, d is the diameter, $d_{\max}$ is the maximal diameter, and the size span (ratio of the largest diameter to the smallest one) is very large. This distribution is closely related to the Apollonian packing [17–20].

In this work we explored systematically the effect of both the size span $\lambda = d_{\max}/d_{\min} = \{2, 4, 8, 12, 16, 24, 32\}$ and the exponent $\eta = \{0.1, 0.2, \ldots, 0.9, 1.0\}$, of GSDs of the form

$$\rho(d) = \left(\frac{d - d_{\min}}{d_{\max} - d_{\min}}\right)^{\eta}, \tag{2}$$

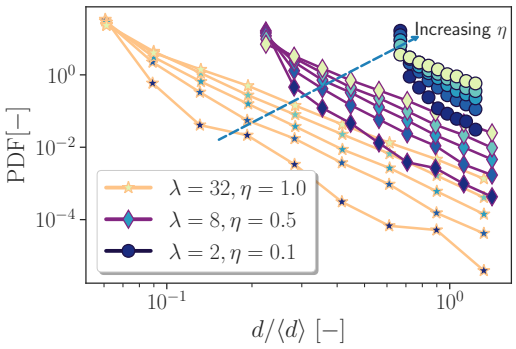

Figure 1. Grain size distributions for three values of λ and $\eta = 01, 0.3, 0.5, 0.7, 1.0$.

where $d_{\min}$ is the minimal diameter. When $\eta = 1$, eq. (2) represents the uniform distribution by volume (i.e., all size classes occupy the same volume). Figure 1 shows several GSDs for different values of λ and η. As it can be seen, these are truncated power laws. In order to generate these samples, the number of particles must vary wildly in order to maintain a maximum difference of 5% between the numerical data and eq. (2). For instance, $\lambda = 2$ required small samples of the order of 10000 particles, while $\lambda = 32$ and $\eta = 0.1$ required almost 500000 particles in 3D (which in turn generated more than 1.5 million contacts).

We studied both 2D and 3D systems, subjected to oedometric (2D) or isotropic (3D) compression [21–24]. The friction is set to zero. This allows to compare the obtained packing fraction values with the typical RCP ($\simeq 0.645$) and the Kepler density ($\simeq 0.74$), to decrease somehow the possible memory efffects on the system, and to focus only on the highest possible fraction that can be attained

*e-mail: wfoquendop@unal.edu.co,william.oquendo@unisabana.edu.co
**e-mail: n.estrada22@uniandes.edu.co

A video is available at https://doi.org/10.48448/xfmd-ay60

by varying inly the GSD. Firstly, we explored the packing fraction ν and the proportion of floating particles κ, as in [25, 26]. Secondly, we studied the force distributions and the relationship between particle size and contact forces. We show that packings with large λ and intermediate values of η produce the densest packings, both in 2D and 3D, confirming Fuller and Thompson findings. We find that for some systems κ can reach values as high as 95%. This means that only a small subset of particles carries the force network. Furthermore, we find that as λ increases the force distribution develops a power-law tail, contrasting with the more typical exponential decay for the strongest forces [27–29].

Samples were compressed oedometrically in 2D and isotropically in 3D. Simulations stopped when the system reached mechanical equilibrium, measured by a small kinetic energy and by a small net force per particle. In 2D, simulations were performed using Contact Dynamics, while in 3D we used soft particle Molecular Dynamics (although with a dimensionless stiffness of $\simeq$ 1000 [22, 30, 31]) with LIGGGHTS [32, 33]. More details can be found in [25, 26, 34].

2 Density and connectivity

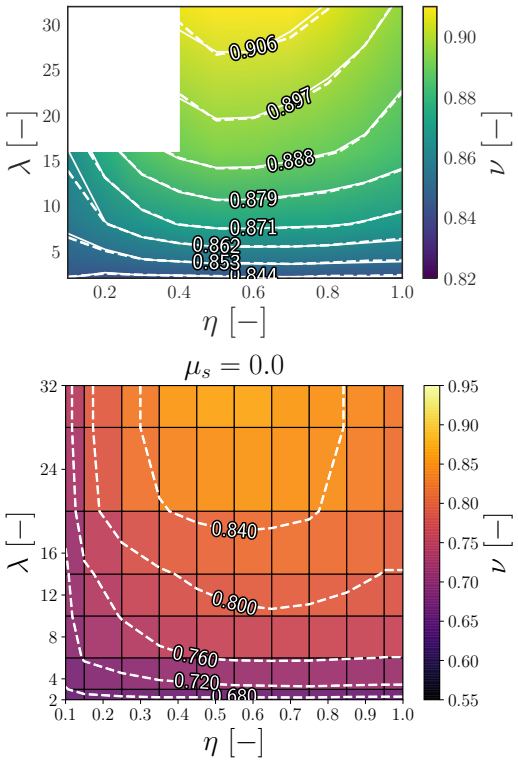

Figure 2. Packing fraction ν as a function of both λ and η. Top: 2D systems under oedometric compression (continuous) and simple shear (dashed lines). Bottom: 3D systems under isotropic compression.

In this section we summarize our results for density and connectivity, in both 2D and 3D [25, 26]. To do so, we use two descriptors: the packing fraction $\nu = V_p/V$, where V_p is the particles volume and V is the sample volume, and the proportion of floating particles $\kappa = N_f/N$, where N_f is the number of floating particles (number of contacts ≥ 2) over the total number of particles N.

Figure (2) shows ν for all λ and η, in both 2D and 3D. It can be seen that there is always a maximum density, which for small λ is found for $\eta = 1$, and for large λ is found for $\eta \simeq 0.5$. This coincides with the Fuller and Thomson results. This happens in both 2D and 3D, confirming that it is an intrinsic result of the GSD. The maximization around $\eta \simeq 0.5$ for large λ is interesting, since that particular GSD can be linked to the well known Apollonian packing. It must be noted that the presented systems are disordered and obtained by means of a mechanical solicitation.

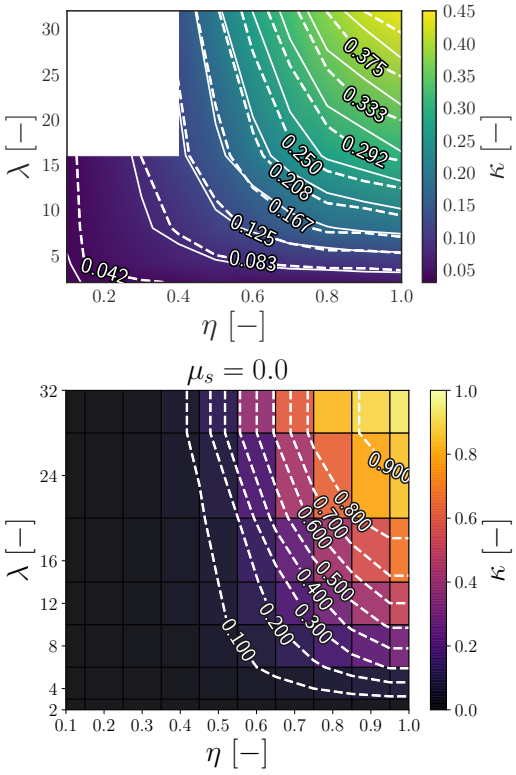

Figure 3. Proportion of floating particles κ as a function of both λ and η. Top: 2D systems under oedometric compression (continuous lines) and simple shear (dashed lines). Bottom: 3D systems under isotropic compression.

Although intermediate values of η produce high densities, the same trend is not found for the proportion of floating particles κ. Actually, there is a monotonic increase in κ for all η, something that is enhanced with increasing λ, as shown in Fig. 3. In 2D systems, κ reaches 40%, for $\lambda = 32$ and $\eta \simeq 1.0$, but in 3D the result are even more impressive, since κ reaches values as high as $\simeq 95\%$. This implies that only 5% of the particles are participating in the force network, which seems extremely low and make those particles susceptible for breaking in a real system. Furthermore, it can be seen that κ is small in the region where $\eta < 0.5$, while it rapidly increases after that, specially in 3D. Therefore, one can say that values for inter-

mediate η produce systems that are both the densest and well connected.

3 Force distributions

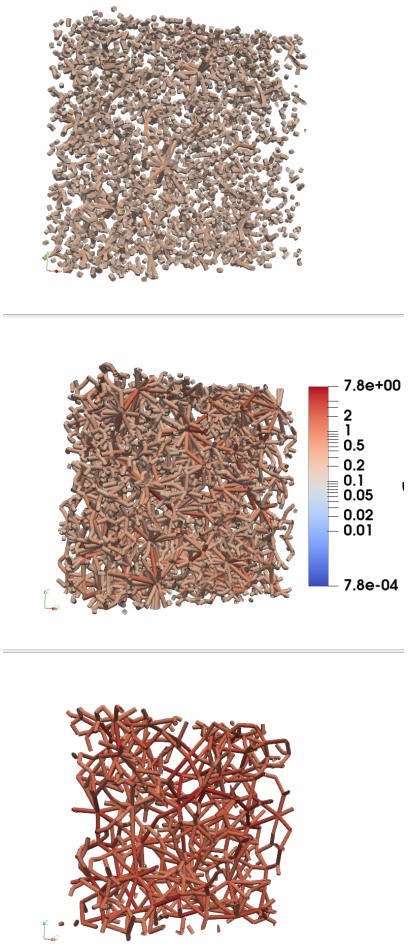

Figure 4. Strong force network for $\lambda = 16$. Top: $\eta = 0.1$, center: $\eta = 0.5$, and bottom: $\eta = 1.0$. Only forces such that $f_n > f_{n,\max}/3$ are shown.

The large number of floating particles, specially for 3D systems, implies an important effect of the GSD on the actual connectivity of the samples after reaching mechanical equilibrium. Figure 4 shows an internal view of the strong force network (only showing forces such that $fn > fn_{\max}/3$), for $\lambda = 16$ and $\eta = 0.1, 0.5, 1.0$. For small η, many particles participate in the force chains, with relatively small forces, while for large η forces concentrate on a small percentage of large particles. for intermediate values of η, the network comprises both small and large particles.

In order to explore how forces are distributed inside the samples, we built the probability density functions of normal forces (PDF). Figure 5 shows the PDFs for all η and for $\lambda = 2, 8, 16, 24$. For large λ, the PDF is well described by a power law, with a tail that grows larger as λ

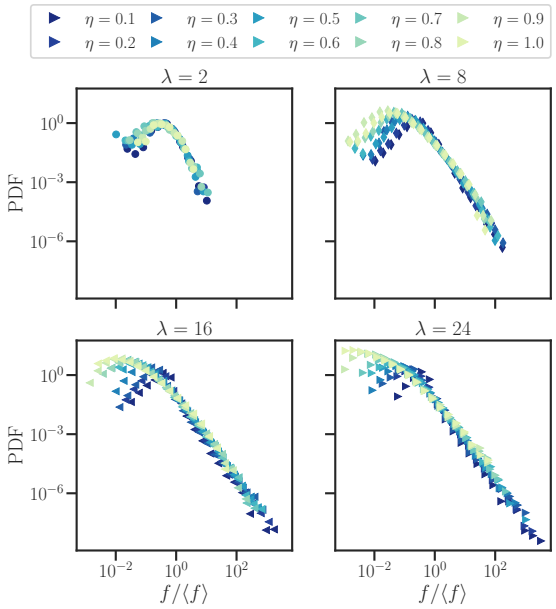

Figure 5. Probability density functions of normal forces, for several λ and all η, in log-log scale.

increases. This contrasts with the usual exponential tail, which seems to be a good description only for small λ.

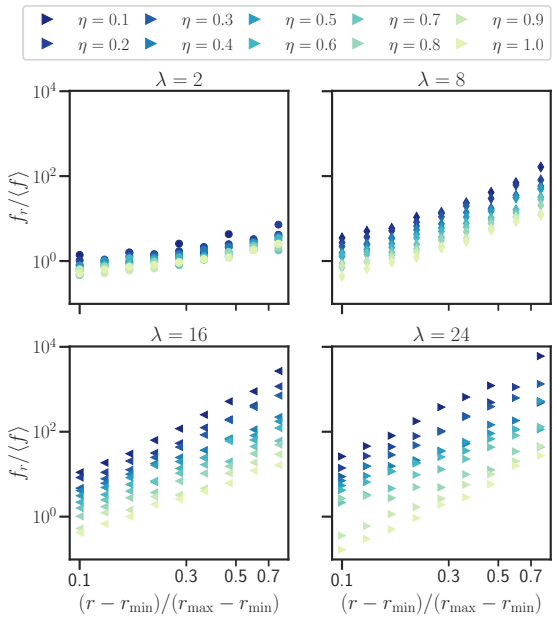

Figure 6. Average force as a function of particle size, for some λ and all η.

Given the large fraction of floating particles for large λ and η, these GSDs must be characterized by some particles supporting very large forces. This suggests a correlation between particle sizes and contact forces. Figure 6 shows the average force $f_{r'}$ as a function of the reduced particle radius $r' = (r - r_{\min})/(r_{\max} - r_{\min})$. It can be seen that $f_{r'}$ increases with r', for all λ and η. The effect is more notorious for large λ, where the relationship is well described by

a power law. These results confirm that large particles effectively support larger forces. This might have important implications on phenomena such as elasticity and particle crushing.

4 Conclusions

In this work we explored the influence of the grain size distribution (GSD), in both 2D and 3D systems, on some packing descriptors such as density, connectivity, and internal forces distributions. By varying systematically the GSD described by eq. (2) and using large size spans (up to 32), we were able to investigate the influence of the GSD on the internal packing structure.

First, we showed that, for compressed systems in oedometric (2D) and isotropic (3D) conditions, there is always an optimal packing for which density is maximized. For large size spans, this optimal packing corresponds to intermediate exponents of the power law GSD, very close to those that characterize the Fuller and Thomson distribution and to the Apollonian packing. Furthermore, by looking at the proportion of floating particles, it was possible to show that the optimal packings are in addition relatively well connected.

Then, we analyzed the distributions of normal forces, finding a power law tail that grows with increasing size span. Furthermore, by plotting the average force as a function of the particle radius it was possible to see that the large particles always carry the largest forces, which is something that might imply higher fracturing probabilities.

These results allow for better understanding the role of the GSD on packings built mechanically, constituting another step towards the prediction of final packing characteristics from GSD properties. Future works could explore the role of friction on both the density and the forces distributions.

References

[1] T. Aste, D. Weaire, *The Pursuit of Perfect Packing, Second Edition* (Taylor & Francis, 2008), ISBN 978-1-4200-6817-7
[2] C. Voivret, F. Radjaï, J.Y. Delenne, M.S. El Youssoufi, Phys. Rev. E **76**, 021301 (2007)
[3] M.R. Shaebani, M. Madadi, S. Luding, D.E. Wolf, Phys. Rev. E **85**, 011301 (2012)
[4] D.H. Nguyen, É. Azéma, F. Radjai, P. Sornay, Phys. Rev. E **90**, 012202 (2014)
[5] N. Kumar, V. Magnanimo, M. Ramaioli, S. Luding, Powder Technol. **293**, 94 (2016)
[6] N. Kumar, S. Luding, Granul. Matter **18** (2016)
[7] C. Voivret, F. Radjaï, J.Y. Delenne, M.S. El Youssoufi, Phys. Rev. Lett. **102**, 178001 (2009)
[8] F. Radjai, J.Y. Delenne, E. Azéma, S. Roux, Granul. Matter **14**, 259 (2012)
[9] A. Santos, S.B. Yuste, M. López de Haro, G. Odriozola, V. Ogarko, Phys. Rev. E **89** (2014)
[10] D.H. Nguyen, E. Azéma, P. Sornay, F. Radjai, Phys. Rev. E **91**, 032203 (2015)
[11] D. Cantor, E. Azéma, P. Sornay, F. Radjai, Phys. Rev. E **98** (2018)
[12] F.W. Taylor, S.E. Thompson, *A Treatise on Concrete, Plain and Reinforced* (John Wiley & Sons, 1905)
[13] W.B. Fuller, S.E. Thompson, T. Am. Soc. Civ. Eng. **59**, 67 (1907)
[14] A.N. Talbot, F.E. Richart, Bulletin 137, University Of Illinois, University of Illinois, Urbana (1923)
[15] C. Furnas, Tech. Rep. Serial No. 2894, Department of Commerce, Bureau of Mines, Report of Investigation Serial No. 2894 (1929)
[16] C. Furnas, Ind. Eng. Chem. **23**, 1052 (1931)
[17] S.S. Manna, H.J. Herrmann, J. Phys. A-Math. Gen. **24**, L481 (1991)
[18] S. Manna, Physica A **187**, 373 (1992)
[19] H. Herrmann, R. Mahmoodi Baram, M. Wackenhut, Physica A **330**, 77 (2003)
[20] F. Varrato, G. Foffi, Mol. Phys. **109**, 2663 (2011)
[21] GDR MiDi, Eur. Phys. J. E **14**, 341 (2004)
[22] I. Agnolin, J.N. Roux, Phys. Rev. E **76**, 061302 (2007)
[23] I. Agnolin, J.N. Roux, Phys. Rev. E **76**, 061303 (2007)
[24] I. Agnolin, J.N. Roux, Phys. Rev. E **76**, 061304 (2007)
[25] N. Estrada, W.F. Oquendo, Phys. Rev. E **96**, 042907 (2017)
[26] W.F. Oquendo-Patiño, N. Estrada, Granul. Matter **22**, 75 (2020)
[27] R.K. Desu, R.K. Annabattula, Granul. Matter **21**, 29 (2019)
[28] M.A. Cárdenas-Barrantes, J.D. Muñoz, W.F. Oquendo, Granul. Matter **20**, 1 (2018)
[29] F. Radjai, D. Wolf, M. Jean, J. Moreau, Phys. Rev. Lett. **80**, 61 (1998)
[30] S. Luding, Granul. Matter **10**, 235 (2008)
[31] F. Radjaï, F. Dubois, eds., *Discrete Numerical Modeling of Granular Materials* (Wiley-ISTE, New York, 2011), ISBN 978-1-84821-260-2
[32] C. Kloss, C. Goniva, A. Hager, S. Amberger, S. Pirker, Prog. Comput. Fluid Dy. **12**, 140 (2012)
[33] O. Tange, *GNU Parallel 2018* (Ole Tange, 2018), ISBN 978-1-387-50988-1
[34] N. Estrada, Phys. Rev. E **94**, 062903 (2016)